Check for updates

Received: 23 December 2021 | Revised: 10 March 2022 | Accepted: 11 March 2022

DOI: 10.1002/pro.4300

METHODS AND APPLICATIONS

THE PROTEIN SOCIETY WILEY

Insect cell expression and purification of recombinant SARS-COV-2 spike proteins that demonstrate ACE2 binding

Lucas R. Struble[1] | Audrey L. Smith[1] | William E. Lutz[1] | Gabrielle Grubbs[2] | Satish Sagar[1] | Kenneth W. Bayles[3] | Prakash Radhakrishnan[1,3,4,5] | Surender Khurana[2] | Dalia El-Gamal[1,4] | Gloria E. O. Borgstahl[1,4,5]

[1]Eppley Institute for Research in Cancer and Allied Diseases, University of Nebraska Media Center, Omaha, Nebraska, USA

[2]Division of Viral Products, Center for Biologics Evaluation and Research (CBER), FDA, Silver Spring, Maryland, USA

[3]Department of Pathology and Microbiology, University of Nebraska Medical Center, Omaha, Nebraska, USA

[4]Fred and Pamela Buffet Cancer Center, University of Nebraska Medical Center, Omaha, Nebraska, USA

[5]Department of Genetics, Cell Biology and Anatomy, University of Nebraska Medical Center, Omaha, Nebraska, USA

Correspondence
Gloria Borgstahl, University of Nebraska Medical Center, 986805 Nebraska Medical Center, Omaha, NE 68198.
Email: gborgstahl@unmc.edu

Funding information
Fred and Pamela Buffett NCI Cancer Center Support, Grant/Award Number: P30CA036727

Review Editor: John Kuriyan

Abstract

The COVID-19 pandemic caused by SARS-CoV-2 infection has led to socio-economic shutdowns and the loss of over 5 million lives worldwide. There is a need for the identification of therapeutic targets to treat COVID-19. SARS-CoV-2 spike is a target of interest for the development of therapeutic targets. We developed a robust SARS-CoV-2 S spike expression and purification protocol from insect cells and studied four recombinant SARS-CoV-2 spike protein constructs based on the original SARS-CoV-2 sequence using a baculovirus expression system: a spike protein receptor-binding domain that includes the SD1 domain (RBD) coupled to a fluorescent tag (S-RBD-eGFP), spike ectodomain coupled to a fluorescent tag (S-Ecto-eGFP), spike ectodomain with six proline mutations and a foldon domain (S-Ecto-HexaPro(+F)), and spike ectodomain with six proline mutations without the foldon domain (S-Ecto-HexaPro(-F)). We tested the yield of purified protein expressed from the insect cell lines *Spodoptera frugiperda* (Sf9) and *Trichoplusia ni* (Tni) and compared it to previous research using mammalian cell lines to determine changes in protein yield. We demonstrated quick and inexpensive production of functional glycosylated spike protein of high purity capable of recognizing and binding to the angiotensin converting enzyme 2 (ACE2) receptor. To further confirm functionality, we demonstrate binding of eGFP fused construct of the spike ectodomain (S-Ecto-eGFP) to surface ACE2 receptors on lung epithelial cells by flow cytometry analysis and show that it can be decreased by means of receptor manipulation (blockade or downregulation).

KEYWORDS

antigen, BET inhibitor, COVID-19, protein purification, SARS-CoV-2, spike protein

This is an open access article under the terms of the Creative Commons Attribution-NonCommercial-NoDerivs License, which permits use and distribution in any medium, provided the original work is properly cited, the use is non-commercial and no modifications or adaptations are made.
© 2022 The Authors. *Protein Science* published by Wiley Periodicals LLC on behalf of The Protein Society.

1 | INTRODUCTION

Although existing previously, coronaviruses have only had their descriptive name (meaning "crown") since 1962.[1] With a total of 24 similar species in the wild, only seven are known to cause disease in humans.[2–6] Of these seven, the most pathogenic members are severe acute respiratory syndrome coronavirus (SARS-CoV, originating in Guangdong China in 2002), Middle East respiratory syndrome coronavirus (MERS-CoV, originating in the Arabian Peninsula in 2012), and the novel coronavirus that emerged in December of 2019 in Wuhan, China.[4,7] In January of 2020, this new coronavirus was named SARS-CoV-2 as the causative agent of the disease, COVID-19. It is most closely related to SARS-CoV with a genomic sequence identity of 79%.[8,9] On March 11, 2020, a COVID-19 global pandemic was declared by the WHO.[10] As of February 25, 2022, there are 5,911,081 confirmed deaths worldwide due to COVID-19 (https://covid19.who.int/). The progression of the pandemic saw variants of SARS-CoV-2 emerge, some with increased virus transmission resulting in a global spread.[11–15] Currently, the omicron variant (https://www.who.int/en/activities/tracking-SARS-CoV-2-variants/) is responsible for the majority of the infections in the United States (https://covid.cdc.gov/covid-data-tracker/#variant-proportions). The omicron variant shows the potential to be not only more infectious than the delta variant with a higher chance of reinfection amongst previously infected individuals, but can significantly evade immunity achieved through current vaccinations.[16–19] Recent emergence of the fast-spreading Omicron variant has reinvigorated efforts to develop more effective countermeasures against COVID-19.[18] Effective vaccines are available to fight the spread of the disease, but each new variant carries the possibility to evade the immunity offered by existing vaccines. Research into SARS-CoV-2 remains vital to curtail the pandemic.

Coronaviruses are positive sense, single-strand RNA viruses with four structural proteins: spike (S), envelope (E), membrane (M), and nucleocapsid (N).[8,20,21] The S protein forms a homo-trimer with each protein composed of two subunits named S1 (residues 14-685) and S2 (residues 686-1273).[9,21,22] S1 is responsible for the initial binding to the aminopeptidase N segment of the angiotensin-converting enzyme (ACE2) receptor, whereupon it is shed, and the S2 subunit mediates fusion with the target cell membrane.[21,23] This interaction between the S protein and the ACE2 receptor of the host's cells is required for virus entry into the cell. Binding occurs with low nanomolar affinity.[9,21] The S protein is highly glycosylated, allowing it to evade the host organism's immune system by using glycosylation to mask up to 40% of the S protein's surface area.[22,24] Accounting for this potential epitope shielding by glycosylation makes expressing S protein in an expression system that will include such glycosylation of spike protein far more useful for immunological assays.

It has recently been shown that transcription of ACE2 is regulated by bromodomain and extraterminal domain (BET) proteins that bind acetylated residues on histones to recruit transcriptional machinery.[25,26] Inhibitors of BET proteins have been shown to decrease ACE2 expression, spike protein binding, and SARS-CoV-2 infection in lung epithelial cells and cardiomyocytes.[27,28] Anti-ACE2 antibodies can similarly attenuate viral entry and infection through the occupation of ACE2 receptors, thus blocking spike protein binding (i.e., ACE2 receptor blockade).[25] The SARS-CoV-2 envelope protein is additionally known to directly interact with BET proteins, but no associated effects have been reported for viral infection.[26]

With the shift in focus of many laboratories toward COVID-19 research, an efficient and reliable method for purifying large amounts of glycosylated S protein is needed. We chose to use baculovirus-based recombinant spike protein expression in insect cells which provide N-glycosylation that mirrors mammalian cells, albeit with simpler side chains with terminal mannose residues instead of sialic acid residues.[29] Insect cell expression systems offer significant advantages over mammalian cell line expression systems. The proteins from insect cell expression systems can have complex post-translational modifications and show immunogenicity, antigenicity, and biological activity similar to authentic natural proteins. Additional benefits include less expensive media, ease of scalability, vectors that are safe for humans, and a greatly reduced turn-around time from starting a culture to expressing protein.[30] In this paper, we demonstrate the expression of four constructs of the original SARS-CoV-2 S protein ectodomain in insect cells using recombinant baculovirus and purification of each using a simple and robust method (Figure 1).[21,23] The spike protein receptor-binding domain (RBD) enhanced green fluorescent protein (eGFP) fusion construct (S-RBD-eGFP) was designed to be useful for biological studies. It is comprised of the RBD portion of the S protein that includes the SD1 domain (319-591) with eGFP and 12x His tag bound by a TEV cleavable linker domain on the C-terminus. The linked eGFP makes the protein easy to track during purification and gives confidence that the construct is folded correctly, as there is a strong relationship between the correct folding of the C-terminal eGFP chromophore and the absence of the upstream linked protein forming inclusion bodies or aggregating.[31,32] The S-Ecto-eGFP construct is much the same, but with the full-length

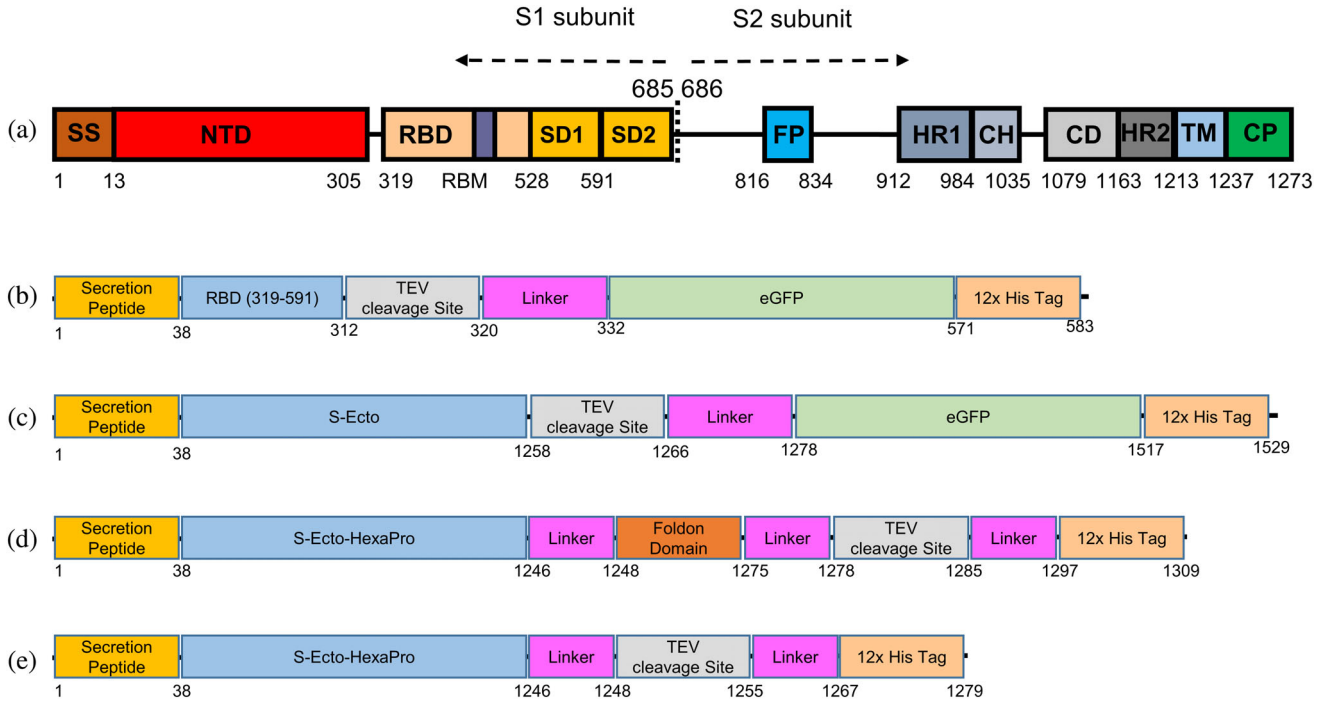

FIGURE 1 Domain map of full-length spike protein and purified Spike constructs. (a) Full-length SARS-CoV-2 spike protein. CD, connector domain; CH, central helix; CP, cytoplasmic peptide; FP, fusion peptide; HR1, heptad repeat 1; HR2, heptad repeat 2; NTD, N-terminal domain; RBD, receptor-binding domain; RBM, receptor-binding motif; SD1/2, subdomain 1 and 2; SS, signal sequence; TM, transmembrane domain. (b) S-RBD-eGFP, (c) S-Ecto-eGFP, (d) S-Ecto-HexaPro(+F), and (e) S-Ecto-HexaPro(-F). Respective domains are insect cell Secretion Peptide (yellow), spike protein (Blue), TEV cleavage site (grey), linker regions (magenta), foldon domain (orange), 12x His Tag (peach)

spike ectodomain replacing the RBD. The S-Ecto-HexaPro(+F) construct is nearly identical to one previously expressed and tested with mammalian expiCHO cells.[33] This construct contains six proline mutations that stabilize the protein, a C-terminal foldon domain to assist with trimerization, and a TEV cleavable 12x His tag attached by a flexible linker region.[34,35] This construct was included in this study to test if the proline mutations will increase protein production in insect cells. The S-Ecto-HexaPro(-F) construct is the same as the S-Ecto-HexaPro(+F) construct, only with the foldon domain removed. This was done to test if the foldon domain has an impact on protein expression levels. All four of the constructs tested had an insect cell secretion peptide added to the N-terminus, and the three ectodomain constructs had the furin cleavage site eliminated (682-685 on S-Ecto-eGFP) by mutation from RRAR to GSAS, preventing S1/S2 subunit cleavage.[4,35] Sequences for all constructs are available in Figure S1.

Each of the purified constructs was tested for binding activity using surface plasmon resonance (SPR), demonstrating that the proteins contain active and functionally folded RBD by their ability to bind ACE2. In addition, we show that the ACE2 receptor blockade or treatment with BET inhibitors (e.g., JQ1 and RVX-208) significantly reduced the binding between the spike protein and ACE2 in cultured human epithelial cells.

2 | RESULTS AND DISCUSSION

2.1 | Purification of spike-ectodomain

The purification of S-Ecto-HexaPro(+F), S-Ecto-HexaPro (-F), S-RBD-eGFP, and S-Ecto-eGFP sequences all follow the same purification protocol. The affinity tag and optional eGFP domain are attached to the S-Ecto and S-RBD domains by a flexible linker that can be cleaved with TEV protease. This cleavage method was chosen because the remaining portion of the TEV protease cleavage sequence (ENLYQ) is not found in the human proteome, and so would not produce a self-recognition epitope in humans. To ensure that the proteins are glycosylated, have high levels of expression, and that the cell culturing was as user-friendly as possible, we chose to express the protein in insect cells using a baculovirus vector. Sf9 and Tni cells were selected for this purpose as Sf9 cells are one of the most widely used for insect cell cultures, while

Tni cells have been shown to express and secrete more recombinant protein than other insect cell lines. The MOI of 5 and incubation time of 3 days was chosen because it resulted in the optimal amount of protein when the media was tested by western blot (not shown).

We tested three types of immobilized metal affinity chromatography (IMAC) resins: Ni-NTA Agarose (Qiagen), Ni Sepharose excel (Cytiva), INDIGO-Ni agarose resin. We found that the cell media leached the nickel ions from the Ni-NTA Agarose resin, significantly reducing the final protein yield. Excel and INDIGO-Ni are both chemical resistant resins, and both showed no observable metal ion leaching. We decided to proceed with our experiments using the INDIGO-Ni resin, as the Excel resin co-purified more impurities (not shown).

We took note of the differences in total protein purified for each construct and each cell line tested (Table 1). The protein yield from 1 L of cultured SF9 cells was 3.5, 0.16, 1.2, and 0.58 mg for S-RBD-eGFP, S-Ecto-eGFP, S-Ecto-HexaPro(+F), and S-Ecto-HexaPro(-F), respectively. The yield from 1 L of cultured Tni cells was 0.2, 4.4, and 1 mg from S-Ecto-eGFP, S-Ecto-HexaPro(+F), and S-Ecto-HexaPro(-F), respectively. S-RBD-eGFP protein yield for Tni cells was not performed. After removal of the affinity tag (or affinity tag + eGFP), 5 μg of each protein was loaded onto SDS-PAGE and stained with SimplyBlue SafeStain. We see all the proteins run at higher molecular weight than what the expected protein size, presumably due to the presence of glycosylation. With the tags removed, S-RBD-eGFP has a calculated MW of 31.6 kDa and runs on SDS-PAGE at 36 kDa, S-Ecto-eGFP has a calculated MW of 136.0 kDa and runs at 160 kDa, S-Ecto-HexaPro(+F) has a calculated MW of 137.9 kDa and runs at 170.0 kDa, and the S-EctoHexaPro (-F) has a calculated MW of 134.6 kDa and runs at 170.0 kDa. The affinity tag (or affinity tag + eGFP) was cleaved from all constructs by TEV protease with varying efficiencies. Using the same type of resin binds the His-tagged TEV protease, cleaved His-tags, spike proteins with intact His-tags, and the non-specifically bound proteins eluted during the first step of purification. This results in extremely pure protein in the flow-through (Figure 2). As tag removal would be required for certain experiments, it is important to be able to cleave the affinity tag from all three subunits of the spike ectodomain as an uncleaved tag on a single subunit will result in all three subunits being removed by the final nickel affinity column and the final protein yield will be reduced.

We tested two types of centrifugal concentrator membranes for their effectiveness in concentrating these proteins: polyethersulfone and regenerated cellulose. We found that all three of the spike ectodomain proteins would bind in a non-recoverable fashion to the polyethersulfone membranes while the S-RBD-eGFP behaved normally. All the proteins tested behaved normally when concentrated with a regenerated cellulose membrane such as the Amicon Ultra 15 (Millipore).

TABLE 1 Protein yield data

Construct	Protein yield from Sf9 cells (mg)	Protein yield from Tni cells (mg)
S-RBD-eGFP (#186)	3.5	NA
S-Ecto-eGFP (#192)	0.16	0.2
S-Ecto-HexaPro(+F) (#314)	1.2	4.4
S-Ecto-HexaPro(-F) (#326)		1

Note: A comparison between yields of recombinant protein purified from 1 L of cell media after purification with a single round of INDIGO Ni agarose resin from both Sf9 cells and Tni cells, as well as the amount of pure protein that could be purified after tag cleavage with TEV protease. The calculated MW values are given alongside the observed MW values for the proteins with tags cleaved. S-RBD-eGFP protein yield in Tni cells was not performed.

2.1.1 | Deglycosylation of the SARS-CoV-2 S-Ecto-eGFP

Spike ectodomain normally has 22 N-glycosylation and 2 O-glycosylation sites (Figure 3).[24,36,37] We explored the type of glycosylation on the purified S-Ecto-eGFP by treatment with N-glycanase (PNGase F), O-glycanase, and Sialidase A. Treatment of S-Ecto-eGFP with N-

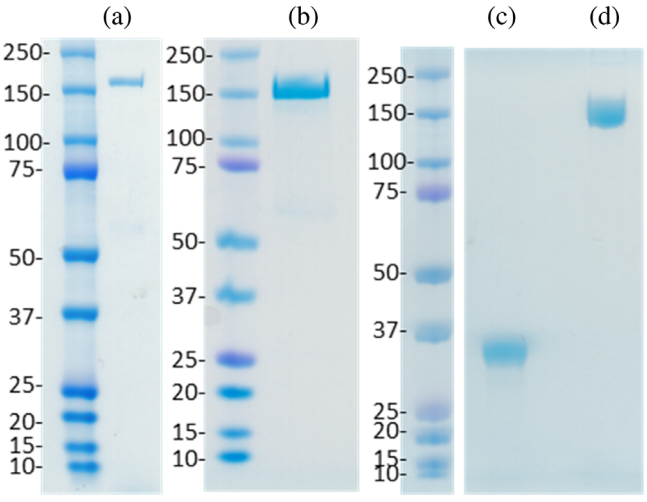

FIGURE 2 SDS-PAGE of fully purified SARS-CoV-2 spike ectodomains and RBD with Affinity tag and eGFP removed. Five microgram of (a) S-Ecto-HexaPro(+F), (b) S-Ecto-HexaPro(-F), (c) S-RBD, and (d) S-Ecto were resolved on 4–12% SDS-PAGE

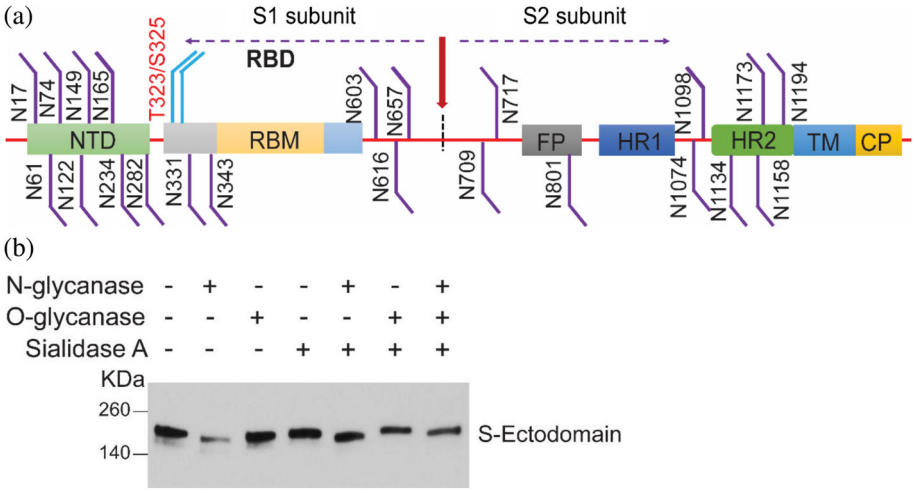

FIGURE 3 Glycosylation of SARS-CoV-2 S-ectodomain. (a) Schematic representation of SARS-CoV-2 S protein's N- and O-linked glycosylation sites. (b) Immunoblotting analysis of Sialidase A, O-glycanase, and N-glycanase treated S-ectodomain

glycanase (PNGase F) showed increased mobility shift and destabilization of the protein due to the loss of heavy N-glycans (Figure 3). However, the treatment of S-Ecto-eGFP with O-glycanase showed a slightly decreased protein mobility shift, which supports the previous findings that S-protein has only two O-linked core-1 derived glycans in its RBD backbone (Figure 3). Conversely, treatment of S-Ecto-eGFP with Sialidase A (which removes sialic acid group) either alone or in combination with either N-glycanase or O-glycanase or together induced a noticeable change in the migration of S-Ecto-eGFP. This decreased mobility shift may be due to the loss of negatively charged sialic acid groups in the N- and O-linked glycans (Figure 3). These results indicate that the SARS-CoV-2 spike protein has both highly sialylated N- and O-linked glycans.

2.1.2 | Binding of the S ectodomain constructs to the hACE2 receptor

The binding of the purified S ectodomains to hACE2 was tested using SPR (Figure 4) to test their activity relative to wild-type proteins made in human 293T cells. The interaction between hACE2 and wild type SARS-CoV-2 spike trimers has a K_D of 14.7 nM.[9,21] The interaction between hACE2 and S-Ecto-eGFP, S-Ecto-HexaPro(+F), and S-Ecto-HexaPro(-F) have K_D values of 55.1, 72.5, and 20.3 nM, respectively. Although the affinity of these purified recombinant proteins to hACE2 is lower (higher K_D), they share the same order of magnitude as the wild type SARS-CoV2 spike trimer indicating that they share a high affinity for hACE2. The binding between wild-type SARS-CoV2 RBD and hACE2 has a K_D of 4.7 nM.[9] The binding between hACE2 and the S-RBD-eGFP construct was 185 nM. This construct binds with only moderate affinity compared to the wild-type SARS-CoV2 RBD. The high-affinity binding of the spike ectodomain constructs and the moderate affinity of the S-RBD-eGFP construct demonstrates that the constructs are properly folded and functionally active like native SARS-CoV-2 spike proteins.

2.1.3 | Targeting ACE2 receptor inhibits binding by the S-Ecto-eGFP

The functional binding of S-Ecto-eGFP to hACE2 on bronchial epithelial Calu-3 cells was additionally evaluated via flow cytometry. Calu-3 cells incubated with S-Ecto-eGFP demonstrated a 2.6-fold greater median GFP fluorescence intensity (MFI) than cells incubated with GFP-His tag control (Figures 5 and 6). Blocking the hACE2 receptor with anti-ACE2 significantly inhibited S-Ecto-eGFP binding compared to IgG control (Figure 5).

Two BET inhibitors were used in this study to down-regulate hACE2 expression on Calu-3 cells.[27] Both JQ1 and apabetalone (RVX-208) significantly inhibited S-Ecto-eGFP binding compared to vehicle control (Figure 6). JQ1 is a pan-BET inhibitor with equal affinity for the two BET bromodomains (BD1 and BD2), while the clinically advanced RVX-208 preferentially targets the BD2 bromodomain. RVX-208 has an established favorable safety profile in clinical trials for cardiovascular indications and is now the focus of a clinical trial for COVID-19 treatment compared to standard of care (Clinical trial identifier: NCT04894266).[28,38,39] In addition to reducing SARS-CoV-2 infection, RVX-208 may play a pivotal role in controlling hyperinflammatory immune responses that can cause long-term tissue damage in patients.[26,28,38,40,41] BET inhibitors have also been reported to decrease the expression of immune inhibitory receptors, such as PD-L1 and LAG3 which hinder T-cell function.[42] High expression of LAG3 correlates with more severe disease

(a)

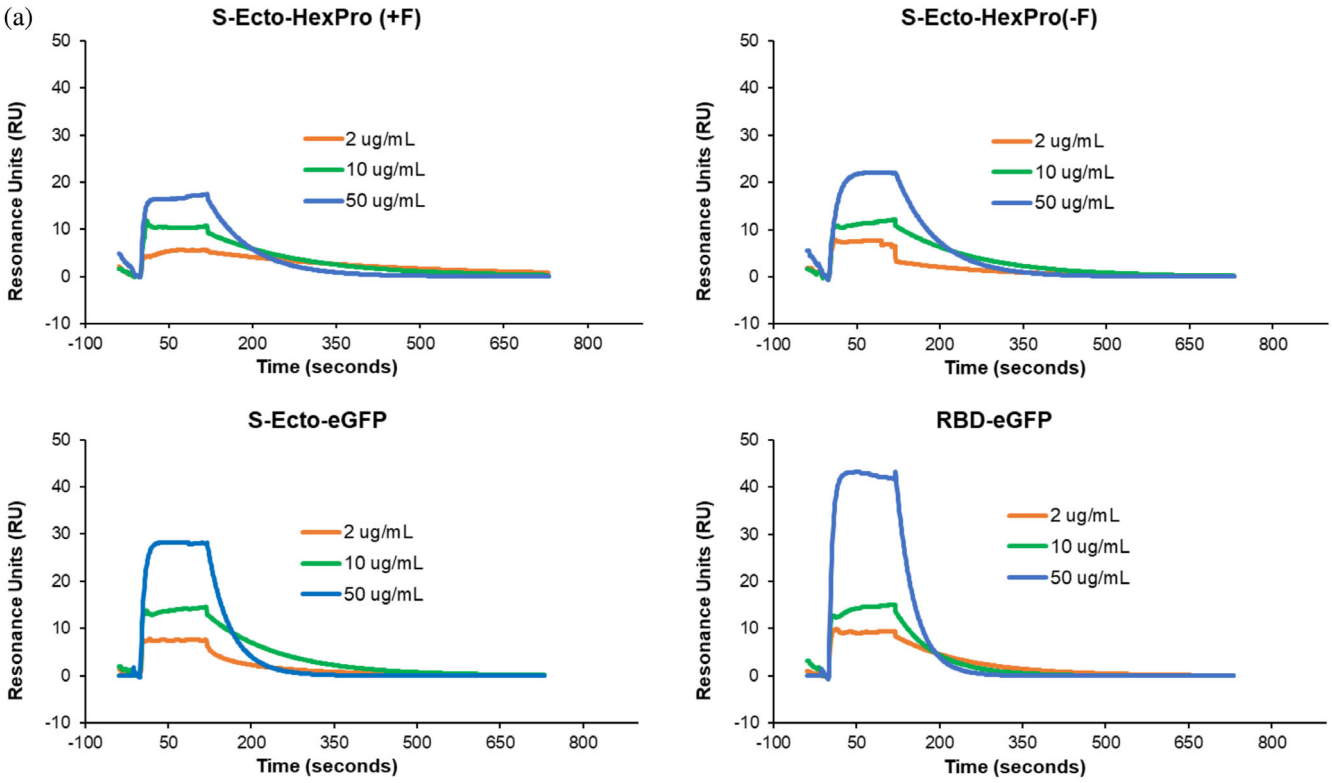

(b)

Protein	K_D (nM)	SD (nM)
S-Ecto-HexaPro(+F)	72.5	7.12
S-Ecto-HexaPro(-F)	20.3	6.77
S-Ecto-eGFP	55.1	2.81
S-RBD-eGFP	185	8.54

FIGURE 4 Activity assessment of purified S-Ecto and RBD constructs for binding to hACE2 protein in SPR. (a) SPR curve-fit plots of spike ectodomain with six proline mutations, with and without a foldon domain ((S-Ecto-HexaPro(+F) and (S-Ecto-HexaPro(-F) respectively), spike ectodomain with eGFP (S-Ecto-eGFP), and spike receptor-binding domain with eGFP (S-RBD-eGFP) at concentrations of 2, 10, and 50 μg/ml binding to hACE2. (b) K_D values with standard deviation (SD) of each recombinant protein binding to hACE2

in COVID-19 patients, with normalization of receptor levels witnessed during recovery.[43]

3 | CONCLUSION

We demonstrated a robust and reliable method for purifying multiple constructs of the S ectodomain that is easy to replicate and can be adapted to different variants of the spike domain to obtain purified active proteins. For all constructs tested, we found that the overall yield was higher when Tni cells were used, with the S-Ecto-HexaPro(+F) specifically showing a large 3.7× increase in yield. Compared to the similar construct expressed in mammalian FreeStyle 293-F cells by Hsieh et al.,[33] we find that the mammalian cell system has a 2.3× increase in yield over our method; however, the ease of culturing insect cells over mammalian cells may prove appealing. Our research also shows the importance of the six stabilizing proline mutations in insect cells, as the yield from Tni cells of S-Ecto- HexaPro(-F) and S-Ecto-HexaPro(+F) constructs showed a 5× and 22× increase, respectively when compared to S-Ecto-eGFP. It is, however, possible that the change in yield is due to the additional eGFP being produced. These results closely match what was seen by Hsieh et al.,[33] where spike ectodomain with the same HexaPro as our constructs was seen to have 10-fold higher expression as a two proline mutant, and the two proline mutant was developed to have higher and more stable expression than the native spike ectodomain.[21] When our results are compared to other published methods for producing full-length spike ectodomain, we find that Wrapp et al.[21] using FreeStyle 293 cells had a yield of 0.5 mg/L, while Hsieh et al.[33] using ExpiCHO

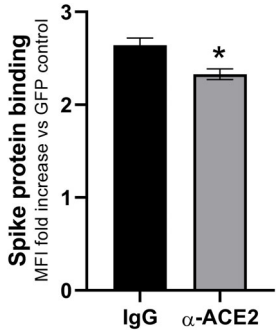

FIGURE 5 Functional S-Ecto-eGFP binding is reduced by ACE2 receptor blockade. Calu3 cells were incubated with 40 μg/ml α-ACE2 or goat IgG antibody (IgG) for 45 min prior to incubation with the S1-ectodomain-eGFP protein. Data are represented as the fold increase of GFP MFI (median fluorescent intensity) compared to GFP-His tag control (mean ± *SEM*). $N = 4$ independent experiments. $^{*}p < .05$

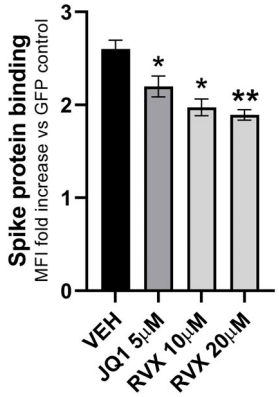

FIGURE 6 Reduced functional S-Ecto-eGFP binding to surface ACE2 in BET-inhibitor treated Calu3 cells. Calu3 cells were treated with BET inhibitors (JQ1, RVX-208; RVX) or control DMSO vehicle (VEH) for 24 hr prior to incubation with the S1-ectodomain-eGFP protein. Data are represented as the fold increase of GFP MFI (median fluorescent intensity) compared to GFP-His tag control (mean ± *SEM*). $N = 3$–4 independent experiments. $^{*}p < .05$, $^{**}p < .001$

cells had a yield of 32.5 mg/L. We find our yields closest to Wrapp et al.,[21] with lower yields using S-Ecto-eGFP (0.16 mg/L from SF9 cells and 0.2 mg/L from Tni cells) and higher yields with S-Ecto-HexPro(+F) (1.2 mg/L with Sf9 cells and 4.4 mg/L with Tni cells) and S-Ecto-HexPro(-F) (0.58 mg/L with Sf9 cells and 1.0 mg/L with Tni cells). The yield for all of our constructs was lower than what was reported by Hsieh et al.[33] When we compare our S-RBD-eGFP construct to our previously published RBD with maltose-binding protein tag (RBD-MBP) expressed in *Escherichia coli* BL21(DE3) cells using CyDisCO to form the required disulfide bonds, we find that our method yields 3.5 mg/L using Sf9 cells opposed to the 0.5 mg/L using the *E. coli* system, and the S-RBD-eGFP construct is likely glycosylated.[44]

As new SARS-nCoV-2 variants continue to emerge, future studies adding to the body of research about the novel coronavirus as well as the development of countermeasures against the COVID-19 disease itself will be required. The process demonstrated provides an entry for small laboratories to begin research into SARS-CoV-2 S protein in vitro or in vivo studies, as well as a rapid start-up for laboratories that are already working in the field.

We also demonstrated that the novel S-Ecto-eGFP construct could be used to measure changes in functional SARS-CoV-2 spike protein binding to commonly infected cells, such as those of the lung epithelium. S1-Ecto-eGFP binding, quantified by flow cytometry, is significantly decreased by blocking the ACE2 receptor with ACE2 antibodies or by reducing ACE2 expression with BET inhibitors. This is relevant because S-Ecto-eGFP functionality can be monitored through ACE2 receptor binding, and we see a decrease in binding as a dose-dependent response to these inhibitors.

Further, the S-Ecto-eGFP construct has already successfully been used in a published study concerning the effect of bromelain on lessening the interaction between the S-Ecto-eGFP and VeroE6 cells and the diminished levels of SARS-CoV-2 infection in VeroE6 cells.[45] In that study, the S-Ecto-eGFP construct was used for multiple experiments that included assessing ACE2 receptor binding, a serological assay where the S-Ecto-eGFP is recognized by COVID-19 positive patient samples, and treatment with bromelain testing for susceptibility to cleavage by the protease.

4 | METHODS

4.1 | Virus creation

The four spike protein sequences were ordered from GenScript in pET28a vectors: S-Ecto-HexaPro(+F), S-Ecto-HexaPro(-F), S-RBD-eGFP, and the S-Ecto-eGFP (S1). SF9 cells and BestBac 2.0 linearized Baculovirus DNA were acquired from Expression Systems (catalog number 91-200). Using the manufacturer's instructions and the aforementioned plasmids, P0, P1, and (if needed) P2 Baculovirus containing our sequence of interest were created.

4.2 | Protein expression

SF9 (*Spodoptera frugiperda*) and Tni (*Trichoplusia ni*) cells (Expression Systems) were grown in sterile PC flasks

(Thermo Fisher Scientific) using ESF-921 media (Expression Systems), in a shaking incubator with a 2 in. orbit running at 160 RPM at 28°C. The day before infection, the cells were passaged to 1×10^6 cells/ml into ESF-AF media (Expression Systems). When the cells reached 2×10^6 cells/ml the following day, they were infected with the appropriate virus at an MOI of 5 and placed in a separate shaking incubator using the same conditions, whereupon they were left to shake for 72 hr. From this point on, all steps were performed at room temperature (RT) or higher to prevent misfolding of the protein.[46] After 72 hr, one cOmplete ULTRA protease inhibitor tablet (Roche) was dissolved in each liter of media, and the contents of the flasks were centrifuged at 400*g* for 10 min. The supernatant was decanted and centrifuged a second time at 14,000*g* for 30 min. The supernatant was then passed through a sterile filter and stored on the benchtop at RT in sterile conditions.

4.3 | Protein purification

All purification steps are performed on the bench at RT. INDIGO-Ni agarose resin (Cube Biotech) was rinsed with wash buffer (20 mM Tris, pH 8.0, 1 M NaCl), added to the media, and stirred at RT for 3 hr. After stirring, the resin was allowed to settle for 30 min. The media was then decanted and disposed of, and the resin suspended in wash buffer. The suspended resin was added to 30-ml gravity-flow columns (BIO-RAD) and washed with 10 CV of wash buffer. The column was washed with 3 CV of wash buffer containing 20, 40, 60, 80, and 100 mM imidazole were performed sequentially. The imidazole stock solution (1 M) was adjusted to pH 8 with NaOH before use. The protein was eluted with wash buffer containing 500 mM imidazole. Washes and elutions were concentrated using an AMICON Ultra-15100 kDa MWCO centrifugal concentrator (regenerated cellulose membrane, Millipore Sigma) and run on ExpressPlus PAGE gels (GenScript) and stained with SimplyBlue SafeStain (Novex) to confirm the location of the eluted protein. Protein concentration was determined by A_{280} using calculated extinction coefficients based on the amino acid sequence.

4.4 | 12x-His tag removal

Once the fraction with the correct molecular weight (MW) band had been identified, it was incubated with MHT237Δ TEV protease (1 mg of TEV protease for every 10 mg of target protein) either on the benchtop overnight or for 2 hr at 37°C.[47] Once cleavage was complete, the protein was buffer exchanged into the wash buffer, and the sample was incubated with the same amount of INDIGO resin as used in the previous step, gently stirring on the benchtop for 3 h. The mixture was then added to a 30-ml gravity-flow column (BIO-RAD), the column was washed with 3 CV of wash buffer, and the flow-through of this wash was collected. The cleaved 12x-His tags, His-TEV protease, and protein with uncleaved 12x-His tags were eluted from the column with 3 CV of wash buffer with added 500 mM imidazole. Amicon Ultra 15 (Millipore) with an MWCO of either 30 or 100 kDa were used to concentrate samples. The cleaved and uncleaved samples were run on SDS-PAGE to monitor cleavage success. The purity of the 12x-His tag cleaved fraction was confirmed by SDS-PAGE where 5 μg of the protein was loaded onto the gel.

4.4.1 | Deglycosylation of the SARS-CoV-2 S-ectodomain

Removal of N-glycans, O-glycans, and sialic acids from the purified S-ectodomain was performed by using a Deglycosylation kit (Agilent, Santa Clara, CA) as per the manufacturer's instructions. Briefly, 1 μg of S-ectodomain was used for N-glycanase, O-glycanase, and Sialidase A (1 μl/reaction) treatment at 37°C for 3 hr. After treatment, the protein-enzyme mixtures were mixed with 2x Laemmli buffer and boiled at 100°C for 5 min. The mixtures were resolved on 4–20% SDS-PAGE and blotted with PVDF membrane. The membrane was immunoprobed with an anti-spike protein antibody as described.[45]

4.4.2 | SPR-based hACE2-binding assay

A sensor chip was captured with recombinant hACE2-AviTag protein from 293T cells (Acro Biosystems, Newark, DE) followed by injection of 300 μl of freshly prepared serial dilutions of S-Ecto-HexaPro(+F), S-Ecto-HexaPro(-F), S-RBD-eGFP, and S-Ecto-eGFP made with Tni cells (Expression Systems) and passed over it at a flow rate of 50 μl/min (contact duration 180 s) for the association, and disassociation was performed over a 600-s interval. A mock surface and buffer-only injections were used to correct for background signal. Bio-Rad ProteOn Manager (version 3.1) was used for data processing.

4.5 | Chemical compounds

Apabetalone (RVX-208) was a kind gift from Resverlogix Corp. (Edmonton, AB, Canada) and JQ1 was purchased

from Cayman Chemicals. Both compounds were dissolved in dimethyl sulfoxide (DMSO).

4.6 | Cell culture

Human bronchial epithelial Calu-3 cells (a kind gift from Dr. Dickinson, UNMC; originally from ATCC) were maintained at 37°C in a humidified environment enriched with 5% CO2 in Eagle's minimum essential medium (EMEM, ATCC) supplemented with 10% fetal bovine serum (FBS), 100 U/ml penicillin, and 100 μg/ml streptomycin.

4.7 | Spike protein binding

Calu-3 were seeded at ~150,000 cells per well in 24-well plates and allowed to adhere for 24 hr before treatment. Cells were treated with BET inhibitors (5 μM JQ1 or 10–20 μM RVX-208) or vehicle (DMSO) in complete growth medium for 24 hr. For antibody blocking conditions, cells were incubated with 40 μg/ml anti-ACE2 (R&D Systems #AF933) or goat IgG isotype control (R&D AB108C) in PBS/2% FBS for 45 min, rocking at RT. For staining, all test samples were incubated with 50 μg/ml S-Ecto-eGFP or control GFP-His tag protein (Sino Biological) and Zombie NIR Fixable Viability dye (BioLegend) in PBS/2% FBS for 30 min, rocking at RT. Samples were suspended in PBS/2% FBS for flow cytometry analyses.

4.8 | Flow cytometry

S-Ecto-eGFP protein binding to live Calu3 cells was measured using a NovoCyte 2060R flow cytometer and analyzed with NovoExpress version 1.4.1 software (Agilent Technologies).

4.9 | Statistical analysis

Statistical significance was determined through student's *t* tests using GraphPad Prism v9 software (San Diego, CA). Comparisons were done versus isotype or vehicle control, and p values of $<.05$ were considered statistically significant.

ACKNOWLEDGMENTS

This research was supported by the Fred and Pamela Buffett NCI Cancer Center Support Grant (P30CA036727) and its associated COVID19 supplement. The authors thank Jason S. McLellan for providing the sequences for the Spike HexaPro proteins. They also thank Mona Al-Mugotir, Savanna Wallin, and Janani Prahlad for their technical assistance.

AUTHOR CONTRIBUTIONS

Lucas R. Struble: Investigation (equal); methodology (equal); visualization (equal); writing – original draft (equal); writing – review and editing (equal). **Audrey L. Smith:** Investigation (equal); methodology (equal); visualization (equal); writing – original draft (equal); writing – review and editing (equal). **William E. Lutz:** Investigation (equal); methodology (equal); writing – review and editing (equal). **Gabrielle Grubbs:** Investigation (equal); writing – review and editing (equal). **Satish Sagar:** Data curation (equal); formal analysis (equal); investigation (equal); methodology (equal); writing – original draft (equal). **Kenneth W. Bayles:** Funding acquisition (equal); writing – review and editing (equal). **Prakash Radhakrishnan:** Conceptualization (supporting); data curation (equal); formal analysis (equal); investigation (equal); methodology (equal); supervision (equal); writing – original draft (equal). **Surender Khurana:** Investigation (equal); methodology (equal); supervision (equal); visualization (equal); writing – review and editing (equal). **Dalia El-Gamal:** Conceptualization (equal); investigation (equal); methodology (equal); supervision (equal); visualization (equal); writing – review and editing (equal). **Gloria Borgstahl:** Conceptualization (equal); funding acquisition (equal); methodology (equal); supervision (equal); writing – review and editing (equal).

CONFLICT OF INTERESTS

The authors declare no potential conflict of interest.

ORCID

Gloria E. O. Borgstahl https://orcid.org/0000-0001-8070-0258

REFERENCES

1. Hamre D, Procknow JJ. A new virus isolated from the human respiratory tract. Proc Soc Exp Biol Med. 1966;121:190–193.
2. Bonilla-Aldana DK, Holguin-Rivera Y, Cortes-Bonilla I, et al. Coronavirus infections reported by ProMED, February 2000-January 2020. Travel Med Infect Dis. 2020;35:101575.
3. Skariyachan S, Challapilli SB, Packirisamy S, Kumargowda ST, Sridhar VS. Recent aspects on the pathogenesis mechanism, animal models and novel therapeutic interventions for Middle East respiratory syndrome coronavirus infections. Front Microbiol. 2019;10:569.
4. Walls AC, Park YJ, Tortorici MA, Wall A, McGuire AT, Veesler D. Structure, function, and antigenicity of the SARS-CoV-2 spike glycoprotein. Cell. 2020;183:1735.
5. Chen Y, Liu Q, Guo D. Emerging coronaviruses: Genome structure, replication, and pathogenesis. J Med Virol. 2020;92:2249.

6. Paules CI, Marston HD, Fauci AS. Coronavirus infections-more than just the common cold. JAMA. 2020;323:707–708.
7. Ghinai I, McPherson TD, Hunter JC, et al. Illinois C-IT. First known person-to-person transmission of severe acute respiratory syndrome coronavirus 2 (SARS-CoV-2) in the USA. Lancet. 2020;395:1137–1144.
8. Hu B, Guo H, Zhou P, Shi ZL. Characteristics of SARS-CoV-2 and COVID-19. Nat Rev Microbiol. 2021;19:141–154.
9. Lan J, Ge J, Yu J, et al. Structure of the SARS-CoV-2 spike receptor-binding domain bound to the ACE2 receptor. Nature. 2020;581:215–220.
10. World Health Organization, WHO Director-General's Opening Remarks at the Media Briefing on COVID-19--March 11, 2020; 2020 Available from: https://www.who.int/director-general/speeches/detail/who-director-general-s-opening-remarks-at-the-media-briefing-on-covid-19—11-march-2020.
11. Soliman MS, AbdelFattah M, Aman SMN, Ibrahim LM, Aziz RK. A gapless, unambiguous RNA metagenome-assembled genome sequence of a unique SARS-CoV-2 variant encoding spike S813I and ORF1a A859V substitutions. OMICS. 2021;25:123–128.
12. Saif R, Mahmood T, Ejaz A, Zia S, Qureshi AR. Whole genome comparison of Pakistani Corona virus with Chinese and US strains along with its predictive severity of COVID-19. Gene Rep. 2021;23:101139.
13. Giovanetti M, Benedetti F, Campisi G, et al. Evolution patterns of SARS-CoV-2: Snapshot on its genome variants. Biochem Biophys Res Commun. 2021;538:88–91.
14. Lau SY, Wang P, Mok BW, et al. Attenuated SARS-CoV-2 variants with deletions at the S1/S2 junction. Emerg Microbes Infect. 2020;9:837–842.
15. Korber B, Fischer WM, Gnanakaran S, et al. Tracking changes in SARS-CoV-2 spike: Evidence that D614G increases infectivity of the COVID-19 virus. Cell. 2020;182:812–827.
16. Shiehzadegan S, Alaghemand N, Fox M, Venketaraman V. Analysis of the delta variant B.1.617.2 COVID-19. Clin Pract. 2021;11:778–784.
17. Cele S, Jackson L, Khoury DS, et al. Omicron extensively but incompletely escapes Pfizer BNT162b2 neutralization. Nature. 2022;602:654–656.
18. Ferre VM, Peiffer-Smadja N, Visseaux B, Descamps D, Ghosn J, Charpentier C. Omicron SARS-CoV-2 variant: What we know and what we don't. Anaesth Crit Care Pain Med. 2022;4:100998.
19. Garcia-Beltran WF, St Denis KJ, Hoelzemer A, et al. mRNA-based COVID-19 vaccine boosters induce neutralizing immunity against SARS-CoV-2 omicron variant. Cell. 2022;185:457–466.
20. Tai W, He L, Zhang X, et al. Characterization of the receptor-binding domain (RBD) of 2019 novel coronavirus: Implication for development of RBD protein as a viral attachment inhibitor and vaccine. Cell Mol Immunol. 2020;17:613–620.
21. Wrapp D, Wang N, Corbett KS, et al. Cryo-EM structure of the 2019-nCoV spike in the prefusion conformation. Science. 2020;367:1260–1263.
22. Huang Y, Yang C, Xu XF, Xu W, Liu SW. Structural and functional properties of SARS-CoV-2 spike protein: Potential antivirus drug development for COVID-19. Acta Pharmacol Sin. 2020;41:1141–1149.
23. Duan L, Zheng Q, Zhang H, Niu Y, Lou Y, Wang H. The SARS-CoV-2 spike glycoprotein biosynthesis, structure, function, and antigenicity: Implications for the design of spike-based vaccine immunogens. Front Immunol. 2020;11:576622.
24. Watanabe Y, Allen JD, Wrapp D, McLellan JS, Crispin M. Site-specific glycan analysis of the SARS-CoV-2 spike. Science. 2020;369:330–333.
25. Qiao Y, Wang XM, Mannan R, et al. Targeting transcriptional regulation of SARS-CoV-2 entry factors ACE2 and TMPRSS2. Proc Natl Acad Sci U S A. 2020;118:e2021450118.
26. Lara-Urena N, Garcia-Dominguez M. Relevance of BET family proteins in SARS-CoV-2 infection. Biomolecules. 2021;11:1126.
27. Gilham D, Smith AL, Fu L, et al. Bromodomain and extraterminal protein inhibitor, apabetalone (RVX-208), reduces ACE2 expression and attenuates SARS-Cov-2 infection in vitro. Biomedicine. 2021;9:437.
28. Mills RJ, Humphrey SJ, Fortuna PRJ, et al. BET inhibition blocks inflammation-induced cardiac dysfunction and SARS-CoV-2 infection. Cell. 2021;184:2167–2182.
29. Ikonomou L, Schneider YJ, Agathos SN. Insect cell culture for industrial production of recombinant proteins. Appl Microbiol Biotechnol. 2003;62:1–20.
30. Jarvis DL. Baculovirus-insect cell expression systems. Methods Enzymol. 2009;463:191–222.
31. Waldo GS, Standish BM, Berendzen J, Terwilliger TC. Rapid protein-folding assay using green fluorescent protein. Nat Biotechnol. 1999;17:691–695.
32. Poppenborg L, Friehs K, Flaschel E. The green fluorescent protein is a versatile reporter for bioprocess monitoring. J Biotechnol. 1997;58:79–88.
33. Hsieh CL, Goldsmith JA, Schaub JM, et al. Structure-based design of prefusion-stabilized SARS-CoV-2 spikes. Science. 2020;369:1501–1505.
34. Meier S, Guthe S, Kiefhaber T, Grzesiek S. Foldon, the natural trimerization domain of T4 fibritin, dissociates into a monomeric A-state form containing a stable beta-hairpin: Atomic details of trimer dissociation and local beta-hairpin stability from residual dipolar couplings. J Mol Biol. 2004;344:1051–1069.
35. Pallesen J, Wang N, Corbett KS, et al. Immunogenicity and structures of a rationally designed prefusion MERS-CoV spike antigen. Proc Natl Acad Sci U S A. 2017;114:E7348–E7357.
36. Shajahan A, Supekar NT, Gleinich AS, Azadi P. Deducing the N- and O-glycosylation profile of the spike protein of novel coronavirus SARS-CoV-2. Glycobiology. 2020;30:981–988.
37. Zhao P, Praissman JL, Grant OC, Zhao Peng, Praissman Jeremy L., Grant Oliver C., Cai Yongfei, Xiao Tianshu, Rosenbalm Katelyn E., Aoki Kazuhiro, Kellman Benjamin P., Bridger Robert, Barouch Dan H., Brindley Melinda A., Lewis Nathan E., Tiemeyer Michael, Chen Bing, Woods Robert J. & Wells L. (2020). Virus-receptor interactions of glycosylated SARS-CoV-2 spike and human ACE2 receptor. Cell Host & Microbe, 28(4):586–601.e6. http://dx.doi.org/10.1016/j.chom.2020.08.004
38. Tsujikawa LM, Fu L, Das S, et al. Apabetalone (RVX-208) reduces vascular inflammation in vitro and in CVD patients by a BET-dependent epigenetic mechanism. Clin Epigenetics. 2019;11:102.

39. An Open-Label Study of Apabetalone in Covid Infection [NCT04894266], 2021. Available from: https://clinicaltrials.gov/ct2/show/NCT04894266?term=Apabetalone&draw=2&rank=3.
40. Wasiak S, Gilham D, Daze E, et al. Epigenetic modulation by apabetalone counters cytokine-driven acute phase response in vitro, in mice and in patients with cardiovascular disease. Cardiovasc Ther. 2020;2020:9397109.
41. Wasiak S, Dzobo KE, Rakai BD, et al. BET protein inhibitor apabetalone (RVX-208) suppresses pro-inflammatory hyperactivation of monocytes from patients with cardiovascular disease and type 2 diabetes. Clin Epigenetics. 2020;12:166.
42. Ozer HG, El-Gamal D, Powell B, et al. BRD4 profiling identifies critical chronic lymphocytic leukemia oncogenic circuits and reveals sensitivity to PLX51107, a novel structurally distinct BET inhibitor. Cancer Discov. 2018;8:458–477.
43. Herrmann M, Schulte S, Wildner NH, et al. Analysis of co-inhibitory receptor expression in COVID-19 infection compared to acute plasmodium falciparum malaria: LAG-3 and TIM-3 correlate with T cell activation and course of disease. Front Immunol. 2020;11:1870.
44. Prahlad J, Struble LR, Lutz WE, et al. CyDisCo production of functional recombinant SARS-CoV-2 spike receptor binding domain. Protein Sci. 2021;30:1983–1990.
45. Sagar S, Rathinavel AK, Lutz WE, et al. Bromelain inhibits SARS-CoV-2 infection via targeting ACE-2, TMPRSS2, and spike protein. Clin Transl Med. 2021;11:e281.
46. Edwards Robert J., Mansouri K, Stalls V, Manne K, Watts B, Parks R, Janowska K, Gobeil S. M. C., Kopp M, Li D, Lu X, Mu Z, Deyton M, Oguin T. H., Sprenz J, Williams W, Saunders K. O, Montefiori D, Sempowski G. D, Henderson R, Munir Alam S, Haynes B. F, Acharya P. Cold sensitivity of the SARS-CoV-2 spike ectodomain. Nature Structural & Molecular Biology. 2021;28(2):128–131. http://dx.doi.org/10.1038/s41594-020-00547-5
47. Blommel PG, Fox BG. A combined approach to improving large-scale production of tobacco etch virus protease. Protein Expr Purif. 2007;55:53–68.

SUPPORTING INFORMATION

Additional supporting information may be found in the online version of the article at the publisher's website.

How to cite this article: Struble LR, Smith AL, Lutz WE, Grubbs G, Sagar S, Bayles KW, et al. Insect cell expression and purification of recombinant SARS-COV-2 spike proteins that demonstrate ACE2 binding. Protein Science. 2022; 31(5):e4300. https://doi.org/10.1002/pro.4300